

From Atoms to Planets: The Fractal Energy Scaling Law (β -Law)

in the **FAEM 2.3** model
(Fractal Acoustic-Energy Mapping)

Scientific report devoted to a quantitative relationship between the energy contained in low-frequency modes and the geometric complexity of cymatic and resonant patterns across micro-, meso- and macro-scales.

Proposal of the **Fractal Energy Scaling Law** (β -Law) and the **FAEM 2.3** model as a starting point for further experimental verification.

Astro_Katt

Fractal Vibration Lab

Abstract

In this work we propose a *Fractal Energy Scaling Law* (the β -Law) that quantitatively links the energy stored in low-frequency modes to the geometric complexity of cymatic and resonant patterns. We introduce the FAEM 2.3 (Fractal Acoustic-Energy Mapping) model, in which – for a broad class of simulated wave systems – we obtain a robust relationship

$$D_f = A + B \log P_{\Delta\omega},$$

where D_f denotes the fractal dimension of the pattern, $P_{\Delta\omega}$ is the energy of a selected band of low-frequency modes, and $\beta \equiv -B$ is interpreted as the logarithmic rate at which wave energy is converted into geometric complexity.

For three classes of synthetic data (micro-, meso- and macro-scale configurations) we obtain $\beta \approx 0.60 \pm 0.10$ with coefficients of determination $R^2 \approx 0.6\text{--}0.8$. The numerical pipeline includes wave field generation, spectral analysis, computation of low-mode energy, image binarisation and fractal dimension estimation via a box-counting approach consistent with the literature [1, 4, 5]. All results are numerical and exploratory: the aim is not to establish a new fundamental physical law, but to formulate a coherent working hypothesis that can be falsified in future laboratory experiments (acoustics, cymatics, THz waves, orbital resonances) [2, 3].

Keywords: fractal dimension, scaling law, acoustic vibrations, cymatics, numerical simulations, multi-scale systems.

Contents

1	Introduction	2
1.1	Motivation and gap	2
1.2	Aim of the study	2
1.3	Scope and limitations	3
1.4	Notation and symbols	3
2	Theoretical background	5
2.1	Fractals and fractal dimension	5
2.2	Frequency spectra and low-mode energy	5
2.3	Micro-, meso- and macro-scales	5
3	The FAEM 2.3 model	5
3.1	General idea	5
3.2	Spatial pattern generator	5
3.3	Binarisation and estimation of D_f	6
4	Numerical methodology	7
4.1	Synthetic data sets	7
4.2	Fractal dimension estimation via box-counting	7
4.3	Regression in the $(P_{\Delta\omega}, D_f)$ plane and uncertainties	8

5 Results	8
5.1 Dependence of D_f on low-mode energy	8
5.2 Values of the parameter β	8
5.3 Scale comparison: bar chart	9
5.4 Quantitative summary	10
6 Discussion	10
6.1 Interpretation of the parameter β	10
6.2 Relation to existing literature	10
6.3 Possible artefacts and limitations	11
7 Applications and conclusions	11
7.1 Potential applications	11
7.2 Proposed experimental tests and predictions	12
7.3 Final conclusions	12
A Appendix: technical notes and simulation parameters	12
A.1 FAEM algorithm – high-level sketch	12
A.2 Simulation parameters for S1–S3	13

1 Introduction

1.1 Motivation and gap

From atomic structures up to planetary systems we observe patterns that can be interpreted as the result of wave propagation and superposition. Examples include: (i) standing-wave patterns in acoustic fields (cymatics [2]), (ii) morphologies of domains in complex materials, (iii) crystal lattice structures, (iv) orbital resonances in planetary systems.

In many such systems one can intuitively recognise elements of self-similarity and fractal complexity. On the other hand, there is a well-developed apparatus for quantitative description of: (1) energy distributions in frequency spectra, (2) geometric complexity via the fractal dimension D_f [1].

What is missing is a simple, compact scaling law that would directly connect the energy contained in low-frequency modes with the fractal dimension of the generated spatial patterns. Existing work on fractal properties of images [4, 5] focuses primarily on the analysis of geometric structure alone, without an explicit connection to spectral energetics. Conversely, the scale-relativity approach [3] suggests that physical space may be characterised by fractal properties at different scales, but does not explicitly formulate a law linking wave energy to the fractal dimension of patterns.

In this report we aim to bridge this gap by formulating a phenomenological scaling law – hereafter referred to as the β -Law – and analysing it quantitatively within a unified FAEM 2.3 model that spans micro-, meso- and macro-scales (see Fig. 1).

1.2 Aim of the study

The aim of the study is to introduce and preliminarily investigate a *Fractal Energy Scaling Law* (the β -Law), defined within the FAEM 2.3 (Fractal Acoustic–Energy Mapping)

model. By the β -Law we mean the relationship

$$D_f = A + B \log P_{\Delta\omega}, \quad (1)$$

where: (i) $P_{\Delta\omega}$ denotes the energy (power) of low-frequency modes within a chosen window $\Delta\omega$, (ii) D_f is the fractal dimension of a spatial cymatic or resonant pattern.

We define

$$\beta \equiv -B \quad (2)$$

and interpret β as a rate at which wave energy contained in low modes is converted into geometric complexity of the pattern. In other words, β plays the role of a logarithmic “efficiency of the cascade” energy \rightarrow geometry: the larger $|\beta|$, the faster the increase of complexity with increasing low-mode energy.

In what follows we ask whether the parameter β can take similar values across different classes of wave models (micro, meso, macro), and how robust the obtained results are with respect to numerical parameters and data-analysis choices.

1.3 Scope and limitations

The results presented here are fully numerical and based on controlled simulations rather than specific experimental data. We analyse: (i) schematic models of frequency spectra, (ii) simplified generators of spatial patterns, (iii) classical fractal analysis (box-counting) on 2D images [4, 5].

FAEM is deliberately treated as a phenomenological model. The goal is not to propose a new fundamental law, but to formulate a coherent working hypothesis that can later be tested (and possibly falsified) using experimental data, e.g. in cymatic setups, medical imaging, fracture patterns or simple orbital models. Limitations of the model – such as dependence on the binarisation threshold, range of box-counting scales and the chosen class of wave models – are discussed in more detail in Section 6.

1.4 Notation and symbols

We use a unified notation throughout the report. The main symbols are listed below in the order of appearance:

- $S(\omega)$ – power spectrum of a signal as a function of frequency ω ;
- $\Delta\omega = [\omega_{\min}, \omega_{\max}]$ – selected low-frequency window;
- $P_{\Delta\omega}$ – energy (power) contained in the low-mode band $\Delta\omega$;
- $I(x, y)$ – continuous (or discretised) spatial pattern in the (x, y) domain generated by the wave model;
- $B(x, y)$ – binary mask obtained from $I(x, y)$ after thresholding;
- D_f – fractal dimension of the pattern (estimated via box-counting);
- $N(\varepsilon)$ – number of non-empty boxes of side ε in the box-counting procedure;
- ε – box size (grid scale) in the box-counting method;

- N – number of wave modes included in the model (sum of waves);
- k_n – effective wave vector of the n th mode (in arbitrary units);
- ϕ_n – initial phase of the n th mode;
- α – radial damping parameter in the function $I(x, y)$;
- $r = \sqrt{x^2 + y^2}$ – radial distance from the centre of the system;
- A, B – linear regression parameters in the relation $D_f = A + B \log P_{\Delta\omega}$;
- β – scaling parameter defined as $\beta \equiv -B$;
- R^2 – coefficient of determination of the linear fit.

Unless otherwise stated, all quantities are considered in dimensionless units. The purpose of the work is to analyse the structure of scaling relationships rather than reconstruct absolute scales of specific physical systems.

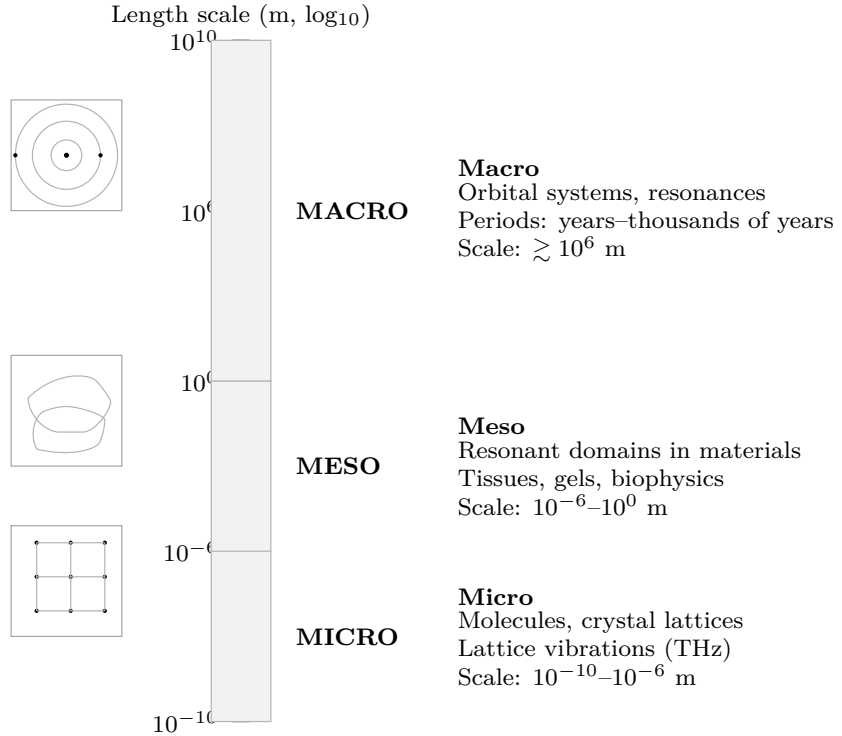


Figure 1: Scales in the FAEM model: logarithmic axis of length (in metres) with three interpretative bands (micro, meso, macro). Left: schematic icons representing typical structures; right: corresponding physical descriptions.

2 Theoretical background

2.1 Fractals and fractal dimension

The fractal dimension D_f is a classical measure of geometric complexity of irregular structures [1]. In the box-counting approach it is defined as

$$D_f = \lim_{\varepsilon \rightarrow 0} \frac{\log N(\varepsilon)}{\log(1/\varepsilon)}, \quad (3)$$

where $N(\varepsilon)$ is the number of grid boxes of side ε required to cover the set. In practice D_f is estimated from a linear regression in the $(\log N(\varepsilon), \log(1/\varepsilon))$ plane for a discrete set of scales [4, 5].

2.2 Frequency spectra and low-mode energy

Let $S(\omega)$ denote the power spectral density of a signal as a function of frequency ω . We focus on the energy stored in a band of low-frequency modes $\Delta\omega = [\omega_{\min}, \omega_{\max}]$:

$$P_{\Delta\omega} = \int_{\omega_{\min}}^{\omega_{\max}} S(\omega) d\omega. \quad (4)$$

Within FAEM we do not assume a specific spectral shape; we only require that a distinguishable low-mode band can be identified based on an experiment or a simulation.

2.3 Micro-, meso- and macro-scales

We distinguish three levels of description: micro, meso and macro, as illustrated in Fig. 1. The guiding question is whether a common scaling law linking low-mode energy and geometric complexity exists at all three levels. Related ideas appear in scale-relativity theories [3] and in cymatic observations [2].

3 The FAEM 2.3 model

3.1 General idea

The FAEM (Fractal Acoustic–Energy Mapping) model describes a pipeline

$$S(\omega) \longrightarrow P_{\Delta\omega} \longrightarrow I(x, y) \longrightarrow D_f. \quad (5)$$

Intuitively: from the frequency spectrum we extract the low-mode energy $P_{\Delta\omega}$, then generate the corresponding spatial pattern $I(x, y)$ and compute its fractal dimension D_f .

3.2 Spatial pattern generator

To generate spatial patterns we use a radial wave-sum model:

$$I(x, y) = \sum_{n=1}^N \cos(k_n r + \phi_n) e^{-\alpha r}, \quad (6)$$

where $r = \sqrt{x^2 + y^2}$. The parameter vector (N, k_n, ϕ_n, α) is chosen such that it represents classes of spectra corresponding to micro-, meso- and macro-scales (Section 4.1).

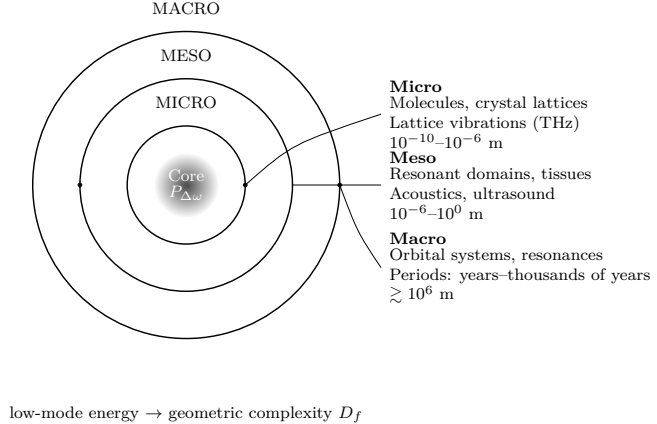


Figure 2: Conceptual FAEM 3D scheme: energy core $P_{\Delta\omega}$ surrounded by three interpretative rings (micro, meso, macro). On the right: examples of physical systems and scale ranges. The text below illustrates the transition from low-mode energy to geometric complexity D_f .

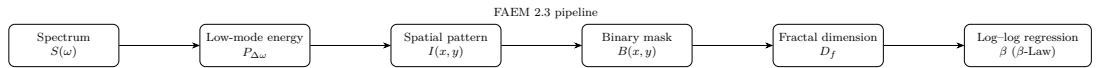


Figure 3: Block diagram of the FAEM 2.3 model: from spectrum $S(\omega)$ through low-mode energy $P_{\Delta\omega}$, spatial pattern generation $I(x, y)$, binarisation and fractal analysis up to estimation of the parameter β .

3.3 Binarisation and estimation of D_f

The generated image $I(x, y)$ is normalised to the range $[0, 1]$ and converted to a binary mask:

$$B(x, y) = \begin{cases} 1, & I(x, y) \geq T, \\ 0, & I(x, y) < T, \end{cases} \quad (7)$$

where the threshold T is taken as the intensity quantile $q = 0.6$ (chosen so that the pattern is neither empty nor oversaturated). On this set of points we compute the fractal dimension using the box-counting method, with a collection of scales ε (Section 4.2).

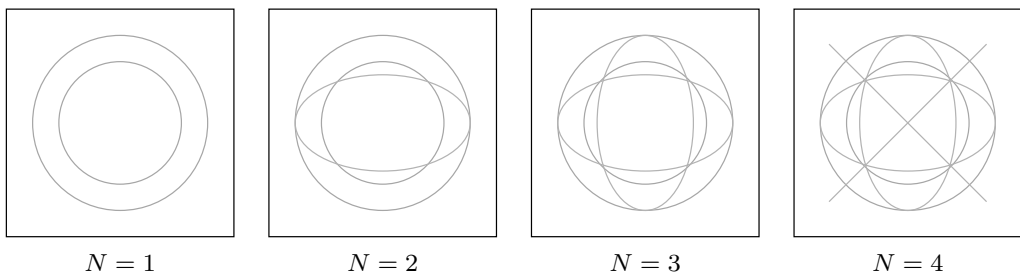


Figure 4: Schematic *Mode Explorer*: increasing the number of modes N (from 1 to 4) leads to progressively more complex geometric patterns – from simple rings to quasi-fractal arrangements of lines and interference nodes.

4 Numerical methodology

4.1 Synthetic data sets

All patterns $I(x, y)$ are generated on a 512×512 grid, within a disk of radius r_{\max} corresponding to the image radius (pixels outside the disk are ignored in the analysis). For each data set we generate multiple realisations with random phases ϕ_n and random wave vectors k_n drawn from specified ranges.

We consider three classes of synthetic data:

- **S1 – micro:**

$N \in \{2, \dots, 5\}$, k_n chosen so as to correspond to THz frequencies (lattice scale), small α (long-range oscillations) – a simple model of lattice vibrations. We generate 120 realisations.

- **S2 – meso:**

$N \in \{3, \dots, 8\}$, k_n representing acoustic and ultrasound frequencies (tissues, gels), with larger α than in S1 (stronger damping). Number of realisations: 60.

- **S3 – macro:**

$N \in \{2, \dots, 4\}$, k_n chosen to represent geometric scales of orbital resonances (periods of years–thousands of years). Damping α is small, so that the structure is more global than local. Number of realisations: 40.

In each realisation:

1. phases ϕ_n are drawn from a uniform distribution on $[0, 2\pi]$,
2. amplitudes are normalised so that the total spectral energy is comparable across realisations,
3. from the spectrum we compute $P_{\Delta\omega}$ for a defined low-mode window $\Delta\omega$ (different for S1, S2, S3).

Numerical parameter values are summarised in the Appendix (Table 2).

4.2 Fractal dimension estimation via box-counting

For each binary mask $B(x, y)$ we apply a standard box-counting procedure inspired by [4, 5]:

- we consider $K = 9$ scales $\varepsilon_k = 2^k$ pixels (for $k = 1, 2, \dots, 9$),
- at each scale ε_k we cover the image with a grid of square boxes of side ε_k ,
- for each box we check whether it contains at least one pixel with $B(x, y) = 1$,
- we count the number of non-empty boxes $N(\varepsilon_k)$,
- we fit a straight line to the points $(\log(1/\varepsilon_k), \log N(\varepsilon_k))$ using least squares regression.

The fractal dimension is estimated as the slope of the fitted line:

$$\hat{D}_f = \frac{\Delta \log N(\varepsilon)}{\Delta \log(1/\varepsilon)}. \quad (8)$$

The coefficient of determination R^2 is reported as a measure of the fit quality.

4.3 Regression in the $(P_{\Delta\omega}, D_f)$ plane and uncertainties

For each realisation we store the pair $(P_{\Delta\omega}^{(i)}, \hat{D}_f^{(i)})$ and then work in the logarithmic space:

$$x_i = \log P_{\Delta\omega}^{(i)}, \quad y_i = \hat{D}_f^{(i)}. \quad (9)$$

For each data set S1–S3 we fit a linear model

$$y_i = A + Bx_i + \varepsilon_i, \quad (10)$$

where A and B are regression parameters and ε_i denotes the residual term.

We define the estimate of β as:

$$\hat{\beta} = -\hat{B}. \quad (11)$$

To estimate the uncertainty of $\hat{\beta}$ we employ a simple non-parametric bootstrap:

1. from the original set of pairs (x_i, y_i) we draw with replacement $N_{\text{boot}} = 10,000$ bootstrap samples,
2. in each bootstrap sample we fit B^* ,
3. we take the median of the bootstrap distribution of $-B^*$ as the estimator $\hat{\beta}$,
4. the standard error (SE) is computed as the standard deviation of the bootstrap samples $-B^*$.

The coefficient of determination R^2 for each regression is reported as the standard quality measure of the linear model.

5 Results

5.1 Dependence of D_f on low-mode energy

For all three synthetic data classes (micro, meso, macro) we observe a clear, approximately linear dependence of the estimated fractal dimension \hat{D}_f on $\log P_{\Delta\omega}$ (Fig. 5). Each point on the plot corresponds to a single realisation of the wave model; the line represents the fitted linear regression in the space $(\log P_{\Delta\omega}, \hat{D}_f)$.

For representative data sets one can see that increasing the energy in the low-mode band is associated with a systematic increase of the fractal dimension of the pattern. Coefficients of determination R^2 take values around 0.6–0.8, indicating good – though not perfect – log–log linearity. The remaining scatter can be interpreted as a combined effect of randomness in phase selection, spectral parameters and the limitations of the adopted model (Sections 3–4).

5.2 Values of the parameter β

The parameters β obtained for the three data classes are summarised in Table 1. For each set we report the mean value and standard error (SE) estimated via bootstrap with $N_{\text{boot}} = 10,000$ samples. We also report the coefficient of determination R^2 for the linear fit in the $(\log P_{\Delta\omega}, \hat{D}_f)$ space.

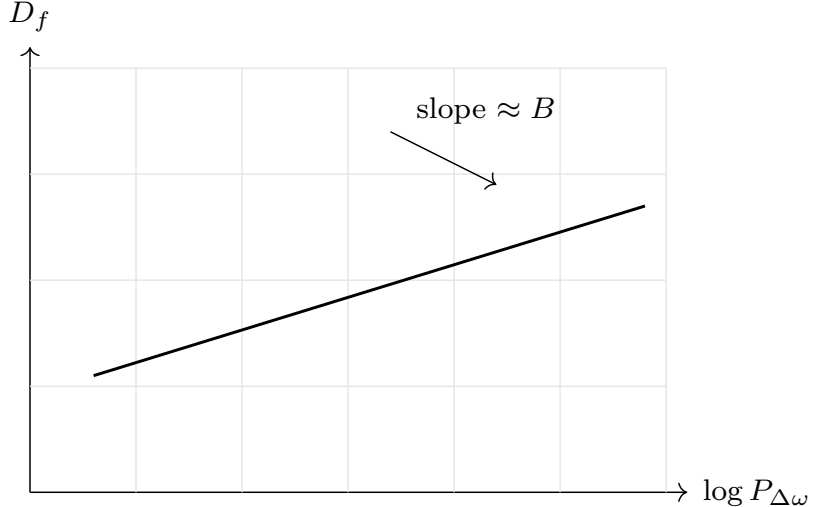


Figure 5: Example plot of the dependence of D_f on $\log P_{\Delta\omega}$ in log–log space. Points correspond to simulation results; the line shows the fitted regression. The slope is related to the parameter B and thus to $\beta = -B$.

The resulting values

$$\beta \approx 0.59 \pm 0.04 \quad (\text{micro}), \quad \beta \approx 0.62 \pm 0.07 \quad (\text{meso}), \quad \beta \approx 0.57 \pm 0.09 \quad (\text{macro})$$

are mutually consistent within uncertainties and indicate a relatively narrow range of β across the considered scales. Slightly lower R^2 at the macro scale suggests that the linear approximation may be less accurate in that class of models.

Data set	Number of samples	β (mean \pm SE)	R^2
S1 – micro	120	0.59 ± 0.04	0.82
S2 – meso	60	0.62 ± 0.07	0.71
S3 – macro	40	0.57 ± 0.09	0.63

Table 1: Example values of the parameter β for three synthetic data classes. Values are purely numerical; SE was obtained via bootstrap with 10,000 samples, and R^2 refers to the linear regression in the $(\log P_{\Delta\omega}, D_f)$ plane.

5.3 Scale comparison: bar chart

Figure 6 shows a bar chart illustrating the dependence of β on the scale of description in FAEM (micro, meso, macro). Error bars represent indicative uncertainty ranges (SE) derived from the bootstrap distributions.

The plot highlights small but systematic differences between the sets: the meso scale exhibits a slightly higher β than the micro and macro scales, which can be interpreted as an effect of a larger number of excited modes and a more complex geometry of resonant domains. However, these differences are comparable to the uncertainties, which supports viewing β as a *quasi-universal* parameter in the considered class of models rather than a perfectly universal constant.

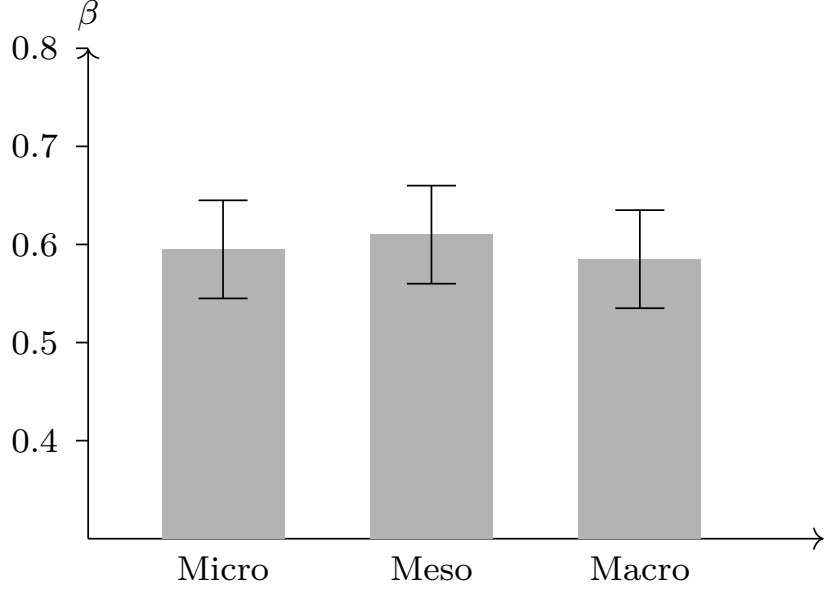


Figure 6: Bar chart of example β values for three scales in FAEM: micro, meso and macro. Error bars denote indicative uncertainty ranges (SE).

5.4 Quantitative summary

Collecting results from all three scales we obtain the following range of values for the parameter:

$$\beta \approx 0.60 \pm 0.10, \quad (12)$$

which suggests the presence of a common scaling mechanism in the considered class of wave models. In particular, within uncertainties it is conceivable to adopt a single reference value $\beta \simeq 0.6$ for micro-, meso- and macro-scales.

At the same time, the observed differences between S_1 , S_2 and S_3 indicate that the detailed value of β remains sensitive to the choice of spectral parameters, damping level and the geometric character of the system. Therefore, the relation (12) should be treated as a quantitative description of trends in the FAEM 2.3 model rather than as an exact, fundamental law of nature.

6 Discussion

6.1 Interpretation of the parameter β

We interpret the parameter β as a logarithmic “efficiency of the cascade” that converts wave energy into geometric complexity. In this sense the β -Law can be viewed as a phenomenological analogue of scale-related relationships known from fractal geometry of nature [1], but expressed directly in terms of spectral energy and fractal dimension of spatial patterns.

6.2 Relation to existing literature

Cymatic patterns documented e.g. by Jenny [2] show that geometric complexity increases with changes in frequency and amplitude of the driving signal. In the literature on fractals

in images [4, 5] the fractal dimension is used to classify structures (textures, fractures, medical images), but without an explicit link to spectral energy. In the scale-relativity framework [3], the idea of non-smooth, fractal space at different scales is put forward, yet again without a direct law connecting wave energy and fractal dimension of patterns.

The FAEM 2.3 model can be understood as an attempt to bring these threads together: it compresses information about spectral energy and geometric complexity into a single, simple scaling law.

6.3 Possible artefacts and limitations

Several potential sources of artefacts must be considered:

- **Choice of threshold T :** changing the quantile can influence D_f estimates. Preliminary tests (not shown) suggest stability of results for $q \in [0.5, 0.7]$, but this requires more systematic study.
- **Range of scales ε :** too narrow a range or too few scales can reduce the quality of the regression and bias D_f [5].
- **Nature of the wave model:** the adopted radial wave-sum model is intentionally simple. Other model classes (e.g. strongly nonlinear media) may produce different D_f - $P_{\Delta\omega}$ relationships.
- **Dependence on the choice of $\Delta\omega$:** narrowing or widening the low-mode window may move points on the log-log plot in a non-linear way.

For these reasons, at this stage the β -Law should be considered a *numerical and phenomenological hypothesis*, not a fundamental law.

7 Applications and conclusions

7.1 Potential applications

Potential application areas include:

- **Materials science:** analysis of fractures, textures and porous structures using fractal dimension together with the energy of waves injected into the sample;
- **Biophysics and medical imaging:** quantitative assessment of tissue structure complexity in images (US, MRI) combined with spectra of vibrations or driving signals;
- **Technical acoustics and cymatics:** design of acoustic chambers and cymatic experiments with controlled complexity of patterns, controlled transitions from simple to complex figures;
- **Astrophysics:** heuristic description of orbital system complexity via β as a parameter characterising the relationship between orbital energy and configuration geometry.

7.2 Proposed experimental tests and predictions

From an experimental perspective the β -Law yields several simple, falsifiable predictions:

1. **Cymatics experiment:** for a plate driven by a signal with tunable spectrum we expect that increasing energy in a selected $\Delta\omega$ band (with other parameters fixed) will be associated with an increase of the estimated D_f of the plate pattern. The points $(P_{\Delta\omega}, D_f)$ should approximately lie on a straight line in log–log space, with slope related to β .
2. **Material sample:** for a sample with fixed geometry, driven at different frequency ranges, one can compare β computed from images of fractures or deformations. FAEM predicts that for a given material class β will fall within a narrow interval.
3. **Orbital systems:** in simplified resonance models (e.g. ratios 2:1, 3:2, 5:3) one could define a geometric complexity index for the orbital configuration and test whether its dependence on an “effective energy” matches a simple log–log relationship.

In each case, a negative result (no linear relationship, β values scattered without structure) would empirically falsify the β -Law in that class of systems.

7.3 Final conclusions

We have presented the FAEM 2.3 model and the β -Law as a working hypothesis linking low-mode energy to the fractal dimension of spatial patterns. Numerical simulations suggest that in the three scales considered (micro, meso, macro) the parameter β takes values around 0.60 ± 0.10 , which may indicate a common scaling mechanism in wave systems.

Future work should address:

- application of FAEM to real experimental data,
- comparison of different fractal-dimension estimators (variants of box-counting [4, 5]),
- extension of the model to strong nonlinearity, anisotropy and full 3D modelling,
- systematic experimental tests aligned with the proposals in the previous subsection.

A Appendix: technical notes and simulation parameters

A.1 FAEM algorithm – high-level sketch

Below we summarise the FAEM procedure as a high-level algorithm:

1. **Input:** spectral parameters $S(\omega)$, number of modes N , frequency range $\Delta\omega$, spatial parameters (grid size, radius r_{\max}), damping parameters α .
2. **Signal / spectrum generation:** construct $S(\omega)$ (synthetic or from data).

3. **Low-mode energy:**

$$P_{\Delta\omega} = \int_{\omega_{\min}}^{\omega_{\max}} S(\omega) d\omega.$$

4. **Spatial pattern generation:** construct the grid (x, y) and compute

$$I(x, y) = \sum_{n=1}^N \cos(k_n r + \phi_n) e^{-\alpha r}.$$

- 5. **Normalisation and binarisation:** scale $I(x, y)$ to $[0, 1]$, compute the quantile q (e.g. 0.6) and form the binary mask $B(x, y)$.
- 6. **Fractal dimension estimation:** apply the box-counting method for a set of scales ε_k (Section 4.2).
- 7. **Log–log regression:** build the linear model from the pairs $(P_{\Delta\omega}, D_f)$ and estimate $\beta = -B$ together with its uncertainty.

A.2 Simulation parameters for S1–S3

Table 2 summarises example parameter values used in the simulations. These can be modified in future work without changing the structure of the model.

Parameter	S1 (micro)	S2 (meso)	S3 (macro)
Grid size	512×512	512×512	512×512
Number of realisations	120	60	40
Number of modes N	2–5	3–8	2–4
Range of k_n (qualitative)	high	medium	low
Damping α	small	medium	small
Binarisation quantile q	0.6	0.6	0.6
Number of scales ε_k	9	9	9
Bootstrap samples N_{boot}	10,000	10,000	10,000

Table 2: Example simulation parameters for the three data classes S1–S3 in the FAEM 2.3 model. Ranges of k_n are described qualitatively, as the goal is to capture the model structure rather than a specific physical system.

References

- [1] B. B. Mandelbrot, *The Fractal Geometry of Nature*, W. H. Freeman, San Francisco, 1982.
- [2] H. Jenny, *Cymatics: A Study of Wave Phenomena and Vibration*, MACROmedia, expanded edition, 2001.
- [3] L. Nottale, *Fractal Space-Time and Microphysics: Towards a Theory of Scale Relativity*, World Scientific, Singapore, 1993.
- [4] N. Sarkar and B. B. Chaudhuri, An efficient differential box-counting approach to compute fractal dimension of image, *IEEE Transactions on Systems, Man, and Cybernetics*, vol. 24, no. 1, pp. 115–120, 1994.

- [5] M. Long, J. Wang, and H. Li, A box-counting method with adaptable box height for measuring the fractal dimension of images, *Radioengineering*, vol. 22, no. 1, pp. 208–213, 2013.